Altered Connectivity of the Balance Processing Network After Tongue Stimulation in Balance-Impaired Individuals

Joe C. Wildenberg,[1,2] Mitchell E. Tyler,[3] Yuri P. Danilov,[3] Kurt A. Kaczmarek,[3] and Mary E. Meyerand[1,3,4]

Abstract

Some individuals with balance impairment have hypersensitivity of the motion-sensitive visual cortices (hMT+) compared to healthy controls. Previous work showed that electrical tongue stimulation can reduce the exaggerated postural sway induced by optic flow in this subject population and decrease the hypersensitive response of hMT+. Additionally, a region within the brainstem (BS), likely containing the vestibular and trigeminal nuclei, showed increased optic flow-induced activity after tongue stimulation. The aim of this study was to understand how the modulation induced by tongue stimulation affects the balance-processing network as a whole and how modulation of BS structures can influence cortical activity. Four volumes of interest, discovered in a general linear model analysis, constitute major contributors to the balance-processing network. These regions were entered into a dynamic causal modeling analysis to map the network and measure any connection or topology changes due to the stimulation. Balance-impaired individuals had downregulated response of the primary visual cortex (V1) to visual stimuli but upregulated modulation of the connection between V1 and hMT+ by visual motion compared to healthy controls ($p \leq$ 1E–5). This upregulation was decreased to near-normal levels after stimulation. Additionally, the region within the BS showed increased response to visual motion after stimulation compared to both prestimulation and controls. Stimulation to the tongue enters the central nervous system at the BS but likely propagates to the cortex through supramodal information transfer. We present a model to explain these brain responses that utilizes an anatomically present, but functionally dormant pathway of information flow within the processing network.

Key words: brain stem; cranial nerve disorders; neural plasticity; statistics; visual system

Introduction

THE VISUAL PROCESSING network encompasses multiple cortical and subcortical structures that communicate to processes the wide variety of visual stimuli we encounter during everyday life (Greenlee and Tse, 2008; Lanyon et al., 2009; McKeefry et al., 2009). This network can be subdivided into separate processing streams for different types of stimulus analysis, such as object recognition and motion processing. Furthermore, these processing streams can pass this information to other networks for use in multisensory integration (Cardin and Smith, 2010; Fetsch et al., 2009; Indovina et al., 2005; Kikuchi et al., 2009).

Cortical processing of motion in the visual field begins with the primary visual cortex (V1), located along the medial occipital lobes (Angelucci et al., 2002; Previc et al., 2000). Partially processed information is passed to the extrastriate visual cortices, including the motion-sensitive visual cortex (hMT+) (Dieterich et al., 2003; Kikuchi et al., 2009; Ohlendorf et al., 2008; Sunaert et al., 1999). If these cortical regions determine that the visual data might contain information pertinent to maintaining balance, other brain regions, including the parieto-insular vestibular cortex (PIVC), the vestibular nuclei, and cerebellar structures, may be recruited to further process and integrate the information (Angelaki and Cullen, 2008; Bense et al., 2005; Bense et al., 2006; Dieterich and Brandt, 2000; Guerraz and Bronstein, 2008; Kovacs et al., 2008; Redfern et al., 2001). The PIVC, located at the parietal-insular junction of the nondominant hemisphere, is one of the least understood regions within this network. It is thought to be a multimodal sensory cortex that integrates visual, vestibular, and proprioceptive information (Brandt and Dieterich, 1999; Eickhoff et al., 2006; Suzuki et al., 2001).

These additional structures work closely with the visual processing network to help maintain balance. Individuals with damage to the sensory inputs and/or neural structures within this network can have deficits of balance and gait, and often experience severe dizziness, nausea, vertigo, and

[1]Neuroscience Training Program, [2]Medical Scientist Training Program, University of Wisconsin, Madison, Wisconsin.
Departments of [3]Biomedical Engineering and [4]Medical Physics, University of Wisconsin, Madison, Wisconsin.

hypersensitive postural responses to motion in their visual field (Baloh and Honrubia, 1990; Borel et al., 2008; Dieterich, 2007; Redfern and Furman, 1994). Multiple imaging studies have investigated abnormal neural processing in this population (Dieterich et al., 2007; Dieterich and Brandt, 2008; Wildenberg et al., 2010). One finding of particular interest is the increased activation of hMT+ bilaterally in some balance-impaired individuals compared to healthy controls (Dieterich et al., 2007). This increased activation may partially explain the increased postural perturbations and subjective hypersensitivity associated with visual motion—especially stimuli that mimic ego-motion (Borel et al., 2008; Redfern and Furman, 1994; Slobounov et al., 2006).

A recent study showed that information-free stimulation to the tongue, termed cranial nerve noninvasive neuromodulation (CN-NINM), can produce sustained reductions in this hypersensitivity to motion in the visual field as measured both behaviorally and through functional magnetic resonance imaging (fMRI) activation (Wildenberg et al., 2010). After the stimulation, balance-impaired individuals displayed improved performance on multiple balance metrics while neuroimaging revealed normalization (compared to healthy controls) of the response of hMT+ to optic flow. The results of that study built on much pre-existing work showing that the tongue can be successfully used as an alternative input for vestibular information by the theories of sensory substitution (Danilov and Tyler, 2005; Danilov et al., 2006; Ptito et al., 2005; Sampaio et al., 2001; Vuillerme and Cuisinier, 2009). The sustained effects discovered in those studies hinted that the stimulation may be inducing plasticity within the network that processes stimuli pertinent to maintaining balance. Activation-based fMRI analysis was able to show that this stimulation likely caused sustained modulation of neural processing within the brainstem (BS) (Wildenberg et al., 2011a). The anatomy of the dorsal medulla/pons supports these findings as the trigeminal nuclei, which receive afferents from the tongue, are located adjacent to the vestibular nuclei.

Those studies, however, were not able to elucidate how modulation of activity within the BS propagates to cortical structures such as the hMT+. Understanding this interaction between brain regions requires a more complex, multivariate analysis that can map information flow through multiple brain regions simultaneously. Effective connectivity methods such as dynamic causal modeling (DCM), structural equation modeling, and Granger causality are common tools to analyze fMRI data in such a way that these complex interactions between brain regions can be mapped (de Marco et al., 2009; Friston et al., 2003; Roebroeck et al., 2005; Schumacker and Lomax, 1996).

The advantages of DCM include the ability to model not only network connections, but also how external perturbations can both drive neural responses in specific regions, and affect connections between these regions. Three different types of interactions are modeled: interconnections between brain regions, activating effects of tasks, and modulation of interconnections by those tasks. DCM also provides a statistical measure to compare models and specific connections between groups (Kasess et al., 2010; Penny et al., 2004; Penny et al., 2010). The purpose of utilizing DCM applied to our previously collected fMRI data was to understand how modulation of structures within the BS due to CN-NINM can cause

global plasticity of the balance-processing network, and better define the potential uses and limitations of this technique in the field of neurorehabilitation.

Methods

Subjects

Twelve subjects selected by common symptoms of chronic balance dysfunction (M/F: 6/6, mean age 52.2 ± 10.3 years) and nine healthy controls (M/F: 5/4, mean age 50.4 ± 12.8 years) participated in this study. Inclusion criteria for the balance-impaired subjects were very broad and included anyone with a clinically defined chronic, stable balance dysfunction that encompassed deficits of balance, posture, and gait (Table 1). Balance-impaired subjects were recruited primarily through referral from clinicians aware of ongoing studies within our research group. These balance-impaired subjects lived throughout the United States and traveled to our facility for participation in the study. Controls were recruited from the general population around Madison, Wisconsin. The University of Wisconsin–Madison Health Sciences Institutional Review Board approved all aspects of this study, and all subjects signed the consent form before participating.

Visual stimuli and display

Two visual stimuli were designed to activate brain regions involved in processing visual information. A static alternating black-and-white checkerboard was used to measure the neural response to any strong visual stimulus. To measure the response to motion in the visual field, subjects were also shown a video that produced the sensation of ego-motion through optic flow. Two-dimensional optic flow was produced by varying the size of the squares at 0.2 Hz in a sinusoidal pattern (apparent in/out motion) and rotating the image about the central point. This rotation was produced using the superposition of two sinusoids (0.2 and 0.35 Hz) after preliminary results indicated that prediction of the rotation produced by a single sinusoid reduced the sensation of ego-motion. The stimuli were displayed for 12 sec alternated with 6 sec of fixation to reduce the contamination of the response from one stimulus into the next.

TABLE 1. DEMOGRAPHIC DETAILS OF THE 12 BALANCE-IMPAIRED SUBJECTS ANALYZED IN THIS STUDY

Subject	Sex	Age	Clinical diagnosis
A	M	56	Central vestibular disorder
B	F	47	Migraine-related balance Disorder
C	M	46	Traumatic brain injury
D	F	46	Chronic Ménière's disease
E	M	38	Spinocerebellar ataxia
F	F	66	Gentamicin ototoxicity
G	M	64	Idiopathic cerebellar ataxia
H	F	43	Spinocerebellar ataxia
I	M	44	Peripheral vestibular disorder
J	F	55	Peripheral vestibular disorder
K	F	51	Idiopathic vestibular disorder
L	M	73	Cerebellar infarction

The clinical diagnosis provided by the referring physician was assumed correct without further testing.

Subjects were shown the visual stimuli in a randomized block-design paradigm with the requirement that each visual stimulus be displayed 14 times over the course of a functional run. Subjects viewed the visual stimuli on MRI-compatible display goggles (Resonance Technology, Northridge, CA) and were instructed to fixate on the center of the image. The goggles produce an 800×600 pixel display with a $30°$ horizontal and $22°$ vertical field of view in each eye.

MRI data collection

MRI data were acquired with the University of Wisconsin–Madison Department of Radiology's 3T clinical MRI scanner (GE Healthcare, Waukesha, WI). T1-weighted anatomical images were collected using a spoiled gradient recalled (3D-SPGR) pulse sequence. Two functional scans were acquired with a T2*-weighted gradient-echo echo-planer imaging sequence (TR = 2000 ms, echo time = 30 ms, flip angle = 75 degrees) to acquire BOLD signal over a 64×64 matrix and 28 axial slices ($3.75 \times 3.75 \times 5$ mm). The first three volumes of each functional scan (252 total volumes) were discarded to allow T1 saturation. Balance subjects underwent two scanning sessions: one before and one after the stimulation regimen. Normal controls underwent one scanning session.

Tongue stimulation

Stimulation to the tongue was delivered via a small electrode array placed on the anterior portion of the tongue and held in place by pressure of the tongue to the roof of the mouth (Kaczmarek, 2011; Tyler et al., 2003). The sensation produced by the array is similar to the feeling of drinking a carbonated beverage. To prevent possible disease transmission, the electrode array was sterilized using gluteraldehyde between subjects and additionally cleaned with 91% isopropyl alcohol between every stimulation session.

CN-NINM stimulation consists of three-square-pulse bursts with an intraburst frequency of 200 Hz and an interburst frequency of 50 Hz that does not vary throughout the duration of the stimulation session. The signal was not coupled to any sensor and therefore did not provide any useful exogenous information to the subject (cf. Danilov et al., 2007, and Danilov et al., 2006, which did provide such feedback).

Procedure

On the day of the first visit (day 0, Pre-CN-NINM and Normal), all subjects underwent behavioral tests and an MRI scan to collect neural responses to the visual stimuli. During the two functional scans, No tongue stimulation was given during the fMRI tests.

CN-NINM stimulation was delivered to the balance subjects over 9 stimulation sessions (two on days 1–4 and one on day 5). During a stimulation session, subjects received continuous stimulation for 20 min, wherein the subject stood as still as possible with their eyes closed. A physical therapist was always present to prevent falls.

After the completion of the ninth stimulation session, balance subjects repeated the fMRI scan. The procedures for the scan on day 5 (Post-CN-NINM) were identical to those completed on day 0. The post-CN-NINM scan was completed between 3 and 6 h after the final stimulation session.

Data preprocessing

MRI data were preprocessed using the AFNI software suite (Cox, 1996). This processing included corrections for slice-time errors and subject motion. No temporal smoothing was performed as DCM utilizes all temporal information to estimate the connectivity between brain regions. An equivalent of spatial smoothing was performed during the DCM time-series extraction step for the regions of interest (below).

The general linear model (GLM) was performed using SPM8 followed by normalization to MNI space for group analysis. Determining the specific effect of visual motion independent of the effect of any visual stimulus would normally be performed using a contrast between the static and dynamic checkerboard tasks (Wildenberg et al., 2010). DCM, however, does not allow contrasts to be used as tasks in the models; therefore, the effect of visual motion had to be explicitly described. To do this, the GLM was organized such that both visual stimuli were combined to measure the effects of any strong visual stimulus (Photic), while only the dynamic stimulus was used to measure the effects of motion in the visual field (Motion). This grouping separated neural responses due to all visual stimuli (Photic) from those that are selective for visual motion without the need for post-hoc contrasts (Penny et al., 2004).

The DCM analysis, performed with SPM8, required multiple procedures beyond the standard GLM approach (Friston et al., 2003). Four clusters, identified by the GLM as responding strongly to the visual stimuli or differing between groups ($p < 0.05$, family-wise error corrected), were selected to be functional volumes of interest (VOIs) for use in the DCM analysis (Fig. 1 and Table 2). These regions included the primary visual cortex (V1), the right motion-sensitive visual cortex hMT+, the right PIVC, and a region within the dorsal
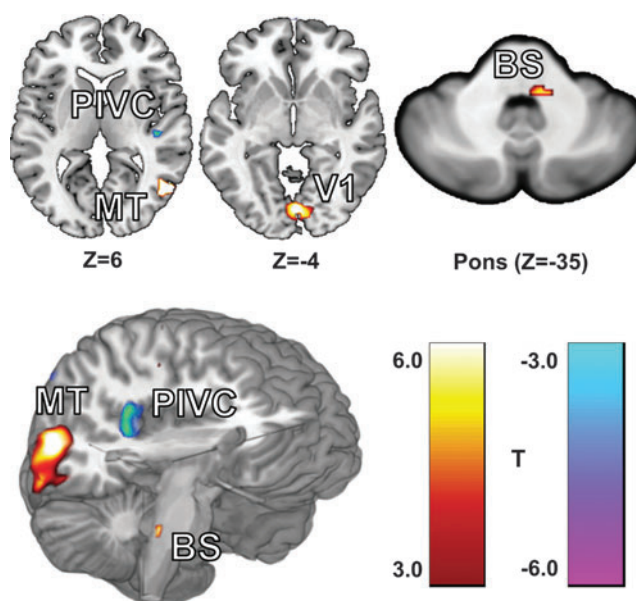
FIG. 1. The locations of the four volumes of interest (VOIs) identified by the group general linear model (GLM) analysis. These four regions showed a strong response to optic flow. Slice locations are given in MNI coordinates and exact center of mass coordinates and volumes are listed in Table 1.

Region	Coordinates	Vol. (µL)	GLM contrast
V1	(5, −83, 0)	9,176	Photic
hMT+	(49, −67, −2)	8,584	Motion
PIVC	(44, −19, 7)	1,520	Motion
BS	(0, −35, −21)	336	Motion (Post-CN-NINM > Pre-CN-NINM)

The coordinates are the center of mass reported in MNI space before reverse normalization. Each VOI is a significant cluster ($p < 0.05$, family-wise error corrected) derived from the specified contrast in the GLM analysis.

VOI, volumes of interest; DCM, dynamic causal modeling; GLM, general linear model; V1, primary visual cortex; hMT+, motion-sensitive visual cortex; PIVC, parieto-insular vestibular cortex; BS, brainstem; CN-NINM, Cranial Nerve Non-Invasive Neuromodulation.

pons of the BS. Only significant voxels ($p < 0.001$, uncorrected) were included in the VOIs. We expected the right and left hemispheres to behave similarly; therefore, the VOI for hMT+ was limited to the right hemisphere (the location of the PIVC) to simplify model analysis and interpretation. The VOI for V1 included voxels from both hemispheres as the cluster produced by the GLM crossed the midline and would have had to be arbitrarily split (Fig. 1). Although defined functionally, it is likely that the BS VOI contains both the vestibular nuclei as well as the trigeminal nuclei—the suspected site of the sustained neuromodulation induced by CN-NINM (Wildenberg et al., 2011a).

Extraction of a representative time-course from each VOI across all subjects required two steps. First, a subject-specific mask of each region (sVOI) had to be produced. These subject-specific masks were created by inverting the subject's normalization transformation matrix (reverse normalization) and applying it to the group VOI masks in MNI space. This step was performed as activation clusters representing the PIVC, and BS regions, corrected for multiple comparisons, were not significant in every subject independently. Only voxels within these sVOIs, in subject space, were considered. Second, principal component analysis (PCA) performed across all voxels in the mask identified the first eigenvariate time-series. These single time-series were used as inputs for the DCM analysis.

DCM model specification

DCM allows three types of influential interactions: interconnections, driving inputs, and modulatory effects. The interconnections describe how separate brain regions influence each other directly. Driving inputs allow tasks to activate brain regions. Finally, modulatory effects allow tasks to affect interconnections. Previous work allowed us to narrow the search space of possible models to estimate. Multiple imaging modalities have shown interconnections between V1 and hMT+ (Greenlee and Tse, 2008; Lanyon et al., 2009). Similarly, previous studies using DCM, as well as knowledge about the function of V1, have implicated visual stimuli as a driving input to V1 (Penny et al., 2004). Therefore, all models included bidirectional interconnections between V1 and hMT+ and a driving input of Photic on V1. All models also include at least one interconnection between hMT+ and the

PIVC, as much data have indicated that these structures communicate (Brandt et al., 1998; Cardin and Smith, 2010).

Using this information, we estimated 50 models that all included the four VOIs and above connections but differed in the remaining interconnections, driving inputs, and modulatory effects. Five of these models included nonlinear interactions, allowing a brain region to modulate an interconnection directly (Stephan et al., 2008). To keep track of all of the possibilities, models were grouped into families defined by the interconnections between regions. The families were first identified by the number of interconnections and then separated based on the specific connectivity of the BS and cortex (Table 3 and Fig. 2A). The models within each of these families differed primarily in the effect of Motion within the network. Motion was allowed to be a driving input, a modulatory effect, or both. These fifty models were calculated across all subjects and functional runs to produce estimations of the connection strengths.

Model selection and averaging

Random-effects Bayesian Model Selection was performed across all models (Penny et al., 2004; Stephan et al., 2009). These calculations produce an estimate of the relative free energy that rewards models for accuracy but penalizes them for increased complexity. Bayesian family inference was also performed to compare the relative strengths of the families (Penny et al., 2010).

The Bayesian family inference suggested that two families of models had the most likely topology (see results). Models from these families were entered into random effects Bayesian Model Averaging (BMA to weigh the strength of each interaction by its relative probability derived from the models which include that interaction) (Kasess et al., 2010; Penny et al., 2010). This procedure uses a Markov chain Monte

Table 3. Names and Descriptions of the Dynamic
Causal Modeling Model Families

Family name	Description	# Models
V1↔BS	V1 interconnections to BS, 5 total interconnections	3
V1↔BS+	V1 interconnections to BS, 6 total interconnections	7
V1↔PIVC	V1 interconnections to PIVC, 6 total interconnections	3
MT↔BS	hMT+ interconnections to BS, 5 total interconnections	7
MT↔BS+	hMT+ interconnections to BS, 6 total interconnections	6
PIVC↔BS	PIVC interconnections to BS, 5 total interconnections	6
PIVC↔BS+	PIVC interconnections to BS, 6 total interconnections	6
Cycle	BS interconnections to both hMT+ and PIVC, 8 total interconnections	7
Nonlinear	Nonlinear effects of BS on other regions' interconnections	5

Families were grouped based on the number of connections as the DCM Bayesian model selection penalizes models with increasing complexity. The groups were further divided by the connection between the brainstem and cortex.
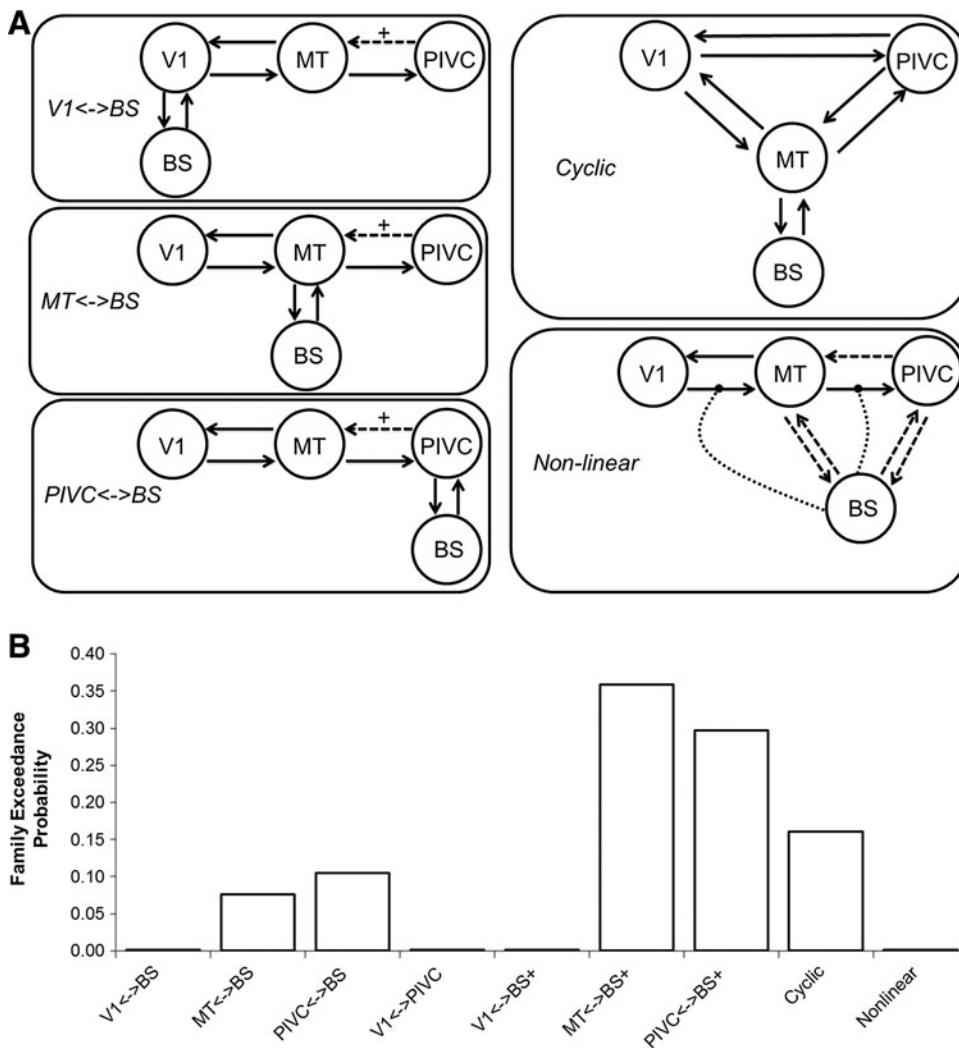
FIG. 2. (A) Topologies for the different model families. The three family groups in the left column are further divided by the presence or absence of the connection from the parieto-insular vestibular cortex (PIVC) to motion-sensitive visual cortex (MT) (dashed line). Those families with this connection have a "+" suffix. The Nonlinear family on the bottom right has several possible connections. The brainstem (BS) region is either connected to MT or the PIVC (but not both), and one modulatory connection from the BS (dotted line). (B) Bayesian family inference of the 50 models separated into nine families based on the interconnections between VOIs. The two highest families, MT↔BS+ and PIVC↔BS+, were entered into Bayesian Model Averaging (BMA) for further analysis.

Carlo technique implemented using a Gibbs sampling algorithm to produce an estimation of the conditional distribution for each interaction weight (Chumbley et al., 2007; DuBois Bowman et al., 2008). The distributions were calculated across all subjects and separately for each group.

To statistically test the distributions for each interaction, one- and two-sample bootstrapping of the mean was performed using all 10,000 samples generated by the Gibbs sampling (Lockhart et al., 2007). Sampling with replacement was performed for 100,000 iterations per connection and group. Each iteration calculated the difference in the means of the resamples to build the distribution for that statistic (Fig. 3). Note that each iteration is not a statistical test by itself, but combine to form the distribution used for statistical testing. The p-value was calculated directly by determining the fraction of the resample distribution greater than the measured difference (Hesterberg et al., 2008). The method is more flexible than a simple t-test as it does not require normality of the distributions or equal variances. However, Gibbs sampling mixes models and subjects, prohibiting a paired comparison of the pre-CN-NINM and post-CN-NINM groups as would normally be performed. To correct for multiple comparisons across the 68 independent tests, only effects with a $p \leq 0.05/68 \sim 0.0008$ are considered significant.

Results

The GLM analysis produced activation clusters at similar locations to those found by our previous analysis (Fig. 1 and Table 2). The preprocessing performed in this study did not include spatial smoothing. Therefore, the locations of the center of mass and the reported volumes differ slightly from the results reported previously (Wildenberg et al., 2010).

Bayesian model selection

Random effects analysis of the 50 models did not produce a single best-fit model across all subjects. Relative probabilities of the model families identified two similar families as being the most likely (Fig. 2B). The 12 models in these two families—MT↔BS+ and PIVC↔BS+—were selected for input into BMA. Note that the next most likely family, cyclic, includes models that are simply combinations of the two families above and are therefore not included in the BMA to reduce redundancy in the calculation.

Bayesian model averaging

Bootstrapping of the samples generated by the BMA revealed multiple significant connections common to all subjects (Table
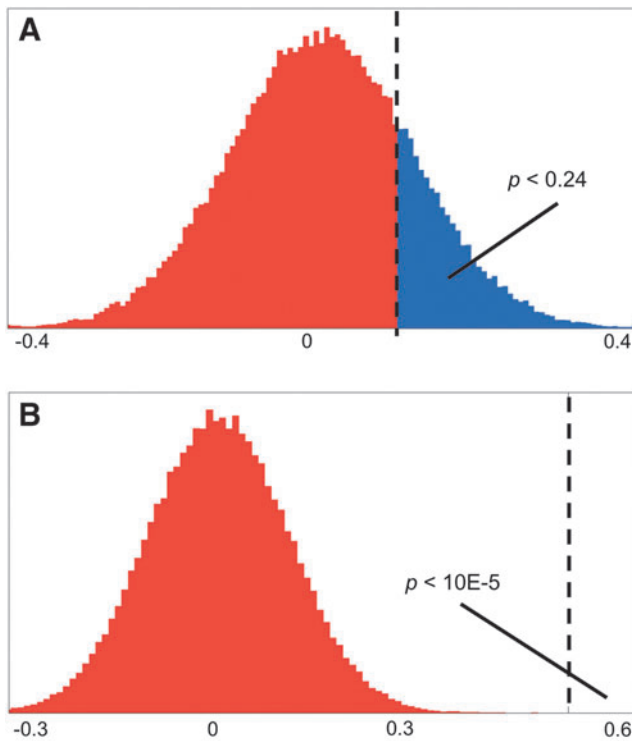
FIG. 3. Example calculation of *p*-values from the bootstrapping procedure. **(A)** Histogram of the difference of the means for the connection V1→hMT+ between pre-Cranial Nerve Non-Invasive Neuromodulation (CN-NINM) and post-CN-NINM. This distribution was calculated using the bootstrapping procedure described in the section Model selection and averaging. The area under the curve greater than the observed difference (0.147–dashed line) is the *p*-value. **(B)** Histogram of the difference of the means for the connection M→ (V1→hMT+) for the same groups. The observed difference (0.05) was much greater than the values from the bootstrap procedure giving a very small *p*-value. The *x*-axes show the difference of the means for each connection.

4). Four interconnections survived corrections for multiple comparisons. V1→hMT+, hMT+→V1, hMT+→PIVC, and hMT+→BS. Both the direct driving effects of Photic→V1 and Motion→BS were also significant. Finally, the modulatory effect of Motion→ (V1→hMT+) was significant.

Bootstrapping to look for differences between groups revealed that balance subjects both before and after stimulation had a smaller driving effect of Photic on V1 compared to healthy controls (Fig. 4 and Table 4). The prestimulation balance-impaired group had a stronger modulatory effect of Motion compared to healthy controls. The strength of this modulation decreased after stimulation resulting in no difference between the balance-impaired individuals post-CN-NINM compared to controls. Last, balance subjects post-CN-NINM had a stronger driving effect of Motion on BS compared to pre-CN-NINM and controls.

Discussion

The baseline interconnections found in this study matched well with what is known about information flow through the network that processes information pertinent to balance

(Albright and Stoner, 1995; Angelucci et al., 2002; McKeefry et al., 2009). Previous studies utilizing DCM to analyze visual processing have identified bilateral connections between V1 and hMT+ (Acs and Greenlee, 2008; Penny et al., 2004). The connection from hMT+ to the PIVC was negative, which matches the simultaneous activation of hMT+ and deactivation of the PIVC found by many studies using optic flow (Cardin and Smith, 2010; Eickhoff et al., 2006; Indovina et al., 2005). The deactivation of the PIVC is only present in the contrast of visual motion to static visual imagery. One interpretation of this finding is a dynamic sensory re-weighting between the visual and vestibular systems that occurs with significant visual motion. This, along with the opposite effect seen with pure vestibular activation, is consistent with the reciprocal inhibitory interaction between these two structures proposed by Brandt and colleagues (1998, 2002). While we did not find an inhibitory connection from the PIVC to hMT+, this is likely due to not including a direct vestibular stimulus (caloric or galvanic) in our experimental paradigm. Finally, there is evidence for direct projections from hMT+ to subcortical structures including the posterior thalamus and pontine nuclei, supporting our finding of a descending connection from hMT+ to the BS (Fries, 1990; Wall et al., 1982).

The direct driving effect of Photic and the modulatory effect of Motion on the connection from V1 to hMT+ have been shown previously using DCM (Penny et al., 2004). These effects are expected, given the hierarchical nature of normal visual processing (Acs and Greenlee, 2008; Cardin and Smith, 2010; Fetsch et al., 2009). The topography of the network in this study (Fig. 5) is consistent with previous investigations into how this network processes sensory stimuli pertinent to maintaining balance (Bense et al., 2006; Brandt et al., 1998; Dieterich and Brandt, 2000; Kikuchi et al., 2009).

In this study, we found that the modulatory effect of Motion on the connection from V1 to hMT+ is upregulated in individuals with balance impairment compared to healthy controls. GLM-based fMRI studies have found increased activation of hMT+ in these subjects in response to optic flow, consistent with the idea that sensory loss in one modality can produce a compensatory increase in the sensitivity of another (Curthoys and Halmagyi, 1995; Dieterich et al., 2007; Wildenberg et al., 2010, 2011b). These connectivity findings support the hypothesis that the motion-sensitive visual cortices are hypersensitive to information arriving from the primary visual cortex.

After CN-NINM stimulation, these same balance-impaired individuals no longer had an upregulated modulatory effect of Motion on the network. This change can be considered a decrease in the weighting of visual motion input to the balance-processing network, consistent with other analyses of this data that showed reduced activation of hMT+ after CN-NINM (Wildenberg et al., 2011b). In particular, this change will result in less PIVC deactivation in response to motion—no longer do strong visual stimuli suppress processing of other sensory modalities (Dieterich and Brandt, 2000; Fetsch et al., 2009; Mahboobin et al., 2005). It is unclear why the direct driving effect of Photic on V1 is decreased in balance dysfunction compared to controls. This effect could represent an attempt to decrease the sensitivity of the entire visual system to compensate for the increased sensitivity to motion.

TABLE 4. MEAN AND p-VALUE OF THE CONNECTIONS ESTIMATED FROM THE BOOTSTRAPPING PROCEDURES

Connection	All subjects		Pre–Norm		Post–Norm		Post–Pre	
	μ	p	$\mu_1 - \mu_2$	p	$\mu_1 - \mu_2$	p	$\mu_1 - \mu_2$	p
V1→MT	−0.028	*	−0.019	0.0012	−0.019	0.0014	0.001	0.8727
MT→V1	0.020	*	−0.002	0.9076	−0.023	0.2307	−0.021	0.2377
MT→PIVC	−0.049	*	0.051	0.0066	0.054	0.0046	0.002	0.8515
PIVC→MT	−0.002	0.4578	0.010	0.6433	0.002	0.9962	−0.008	0.5861
MT→BS	0.025	*	0.005	0.7306	−0.023	0.1461	−0.028	0.0407
BS→MT	0.006	0.0351	−0.005	0.7801	0.018	0.2576	0.023	0.1112
BS→PIVC	−0.001	0.5373	0.005	0.7520	0.005	0.7805	0.000	0.9765
PIVC→BS	0.001	0.6102	0.002	0.8945	0.006	0.7545	0.003	0.8168
M→ (V1→MT)	0.137	*	0.067	*	0.017	0.0186	−0.050	*
M→ (MT+ →PIVC)	−0.001	0.6887	0.001	0.9558	0.000	0.9955	−0.001	0.9525
M→ (MT+ →BS)	0.000	0.9832	0.000	0.9599	0.000	0.9426	0.000	0.9800
M→ (PIVC→MT)	−0.001	0.1300	0.003	0.5274	0.004	0.3851	0.001	0.7782
M→ (PIVC→BS)	0.000	0.9753	0.000	0.9840	0.000	0.9918	0.000	0.9925
M→ (BS→MT)	0.001	0.1218	0.000	0.9424	−0.002	0.6565	−0.002	0.6214
M→ (BS→PIVC)	0.000	0.9749	0.000	0.9885	0.000	0.9224	0.000	0.8862
P→V1	0.638	*	−0.083	*	−0.097	*	−0.014	0.3972
M→BS	0.003	*	0.000	0.3726	0.009	*	0.008	*

Only connections with $p \leq 0.0008$ are significant after correction for multiple comparisons. Only connections that survived the correction for multiple comparisons across all subjects are included in the final model (Fig. 5). Pre, before CN-NINM stimulation; Post, after CN-NINM stimulation; Norm, healthy controls; M, motion; P, photic; μ, mean; *$p \leq 1E-5$.

The results from this study do not indicate exactly how these modulations of cortical neural activity occur; however, they are likely related to the increased driving effect of Motion within the dorsal pons. A high-resolution fMRI study using the same stimulation paradigm and similar subject population presented here suggests that this new response to Motion within the BS is occurring in the trigeminal nuclei, which receive somatosensory afferents from the tongue (Wildenberg et al., 2011a). It is known that there are descending pathways from the superior colliculus to the vestibular nuclei that allow visual-motion information to activate the vestibular complex (Beraneck and Cullen, 2007; Blazquez and Highstein, 2007). Bidirectional connections between the vestibular and trigeminal nuclei have been found using tracer studies, while functional studies have shown that stimulation of one nucleus can modify activity within the other (Anker et al., 2003; Buisseret-Delmas et al., 1999; Herrick and Keifer, 2000; Marano et al., 2005; Satoh et al., 2009). This provides a cellular mechanism by which visual-motion information can reach the trigeminal nuclei. We hypothesize that CN-NINM directly stimulates the trigeminal nuclei and may sensitize them to this incoming information, explaining the stronger response to visual motion poststimulation (Bolognini et al., 2009).
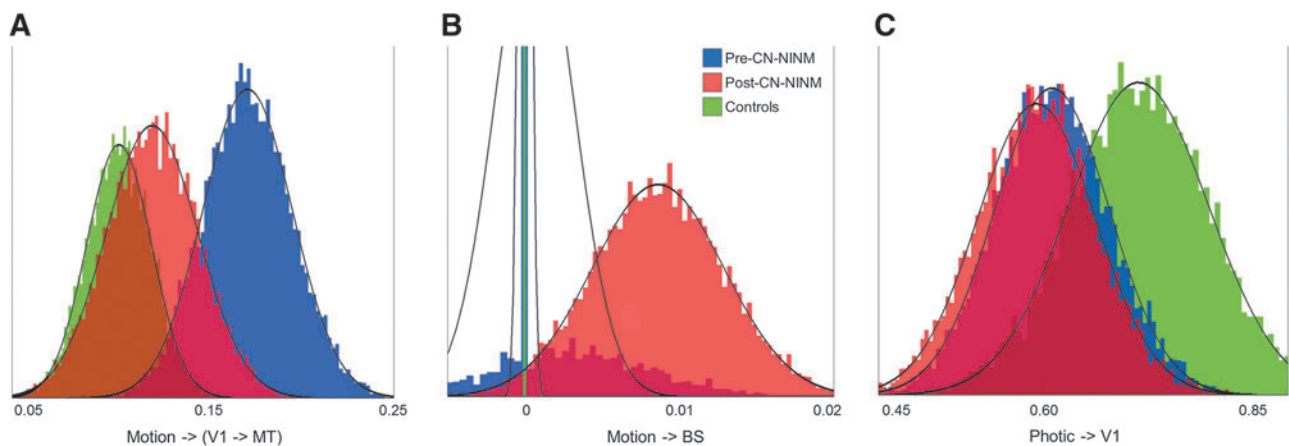
FIG. 4. Histograms of the Gibbs-sampled distributions for the three connections that showed significant group differences in the two-sample bootstrapping (Table 3). It is these distributions that are used in the bootstrapping procedure to determine significance (Fig. 3). (A) The modulatory connection of motion on V1→MT was significantly stronger for balance-impaired individuals before stimulation compared to after stimulation or healthy controls. (B) The direction effect of Motion on the BS region was only seen in individuals after stimulation. (C) Balance-impaired individuals had a smaller driving effect of the Photic visual stimuli on the primary visual cortex V1 than healthy controls. Solid lines are fits to a normal distribution. The x-axes show the difference of the means for each connection.
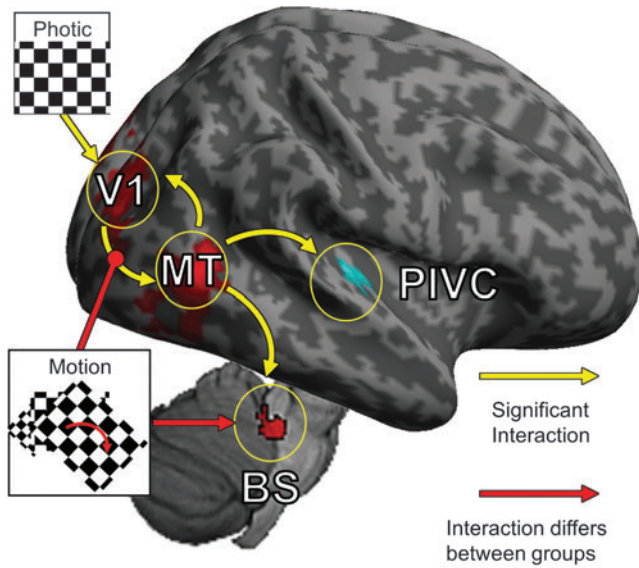
FIG. 5. Diagram of the significant network connections found in this study. Yellow arrows represent connections that were significant but did not differ between groups. Red arrows represent connections in which there was a significant difference between groups. The strengths of all connections are listed in Table 4.

FIG. 6. Diagram of the proposed circuit explaining how CN-NINM stimulation can modify cortical processing of visual motion. Solid lines indicate connections suggested by this study. Dashed lines indicate connections discovered or proposed by the studies listed next to the connection. Proximal structures including the retina, lateral geniculate nucleus, and superior colliculus are not shown. Note that in this study a connection between hMT+ and a functional brainstem region was found, but the difference between the trigeminal and vestibular nuclei could not be resolved. Therefore, this arrow is not included in the proposed circuit. V1, primary visual cortex; hMT+, motion-sensitive visual cortex; VN, vestibular nuclei; TN, trigeminal nuclei; Th, thalamic nuclei.

There are several reports showing that the cortical visual-motion center hMT+ can receive and process motion information acquired via extra-visual modalities, the so-called supramodal sensory flow (Bicchi et al., 2008; Lewis et al., 2000; Matteau et al., 2010; Ricciardi et al., 2007; Sathian, 2005). In particular, studies using a similar tongue stimulation device as used in this study have found activation of hMT+ due to tactile motion on the tongue (Matteau et al., 2010; Ptito et al., 2005). Furthermore, there are data to suggest that this information may not pass through the normal visual pathway, but travel instead directly from the BS, through the thalamus, to hMT+ (Berman and Wurtz, 2010; Lopez and Blanke, 2011; Schoenfeld et al., 2002; Sincich et al., 2004). Although we did not model the thalamic nuclei in this study, it is expected that the thalamus is acting as an intermediate between the BS and cortex. Additional processing by or external effects on the thalamus could explain why the direct connection from the BS to hMT+ was not significant. Future work needs to include this structure, either defined functionally or anatomically, to more accurately model the entire network.

The information from the BS may also affect the cortex through nonlinear interactions. Unlike interconnections, these interactions allow activity within one brain region to modulate the connection between two other regions. It has already been shown that attention to motion in the visual field may exhibit nonlinear modulation of information flow through the visual processing stream (Friston and Buchel, 2000; Stephan et al., 2008). Some of the models included in this study modeled these nonlinear interactions; however, it is possible that, if present, these effects may exist at the level of the thalamus that was not modeled in this study and should be included in more complete models.

These individual pieces of data allow us to hypothesize about the underlying neurobiological mechanism of CN-NINM (Fig. 6). Information about visual motion normally descends to the vestibular nuclei from the thalamus and/or superior colliculus. Stimulation of the tongue induces neuroplasticity in the trigeminal nuclei such that they now respond to this information from the vestibular nuclei. Without passing through V1, this information ascends to the thalamus and then on to hMT+. Activation of this new pathway, even without concurrent stimulation, leads to normalization of activity within hMT+. This sustained alteration of balance processing within the network could explain the reduced postural sway and improvements on functional tests seen in balance subjects after CN-NINM.

The data from the original study and thus the analysis presented here were limited by a lack of control subjects who did not receive CN-NINM stimulation. The time-intensive stimulation procedures prevented recruitment of subjects willing to be assigned to a placebo, while the noticeable sensation of the stimulation on the tongue further reduced the ability to create a true placebo effect. We believe that the chronic nature of the impairments in the included subjects makes spontaneous recovery unlikely. It is possible that some of the observed changes between the first and second scan for the balance-impaired subjects could have been due to increased comfort in the scanner, or other variables such as sleep or caffeine use. We believe that these effects are minimal as all balance-impaired subjects had undergone one (or multiple) clinical MRIs in the course of the workup for their disorder, and it is unlikely that individual factors (sleep, caffeine, etc.) would present at the group level. We also believe the 5-day separation between the pre- and post-fMRI scans eliminated the

possibility of habituation to the visual stimuli as exposure to optic flow is common in everyday life. Future studies are needed to verify that the changes seen in the pattern of neural activity in response to optic flow are indeed due to the stimulation alone.

The results from this study suggest that a cortico-pontine circuit may be responsible for the cortical neuromodulation seen after information-free tongue stimulation. Future directions include connectivity studies that focus on the BS, allowing a differentiation of the different BS nuclei and how balance-pertinent information flows between these nuclei. Subsequent studies also need to include the thalamus that is almost universally involved in communication between cortical and subcortical structures. In addition, a study that incorporates both visual and vestibular stimuli could allow more complete mapping of the dynamic interaction between these two sensory systems.

Conclusion

The network that processes visual motion includes multiple regions and overlaps significantly with the balance-processing network. These many regions must interact properly to process the multiple modalities that provide information pertinent to maintaining balance. Here we have used DCM to map some of the connections between the primary visual cortex (V1), the motion-sensitive visual cortex (hMT+), the PIVC, and a region within the BS that is modulated by CN-NINM tongue stimulation. The results of the analysis confirm previous imaging studies showing hypersensitive responses of hMT+ to visual motion in balance-impaired individuals compared to normal controls. This hypersensitivity is reduced after CN-NINM, and this reduction is likely related to the sustained neuromodulation within the BS. This analysis begins to elucidate how the tongue can be a gateway to the central nervous system (Mandonnet et al., 2010). Finally, we propose a functional neuroanatomical circuit that may explain how electrical stimulation, applied to the tongue, can influence cortical processing of visual motion.

Author Disclosure Statement

Joseph Wildenberg reported no financial or potential conflicts of interest. Authors Danilov, Kaczmarek, and Tyler have an ownership interest in Advanced Neurorehabilitation, LLC, which has intellectual property rights in the field of research reported in this publication. Mary Meyerand reported no financial or potential conflicts of interest.

The content is solely the responsibility of the authors and does not necessarily represent the official views of the National Institute of Diabetes and Digestive and Kidney Diseases or the National Institutes of Health.

References

Acs F, Greenlee MW. 2008. Connectivity modulation of early visual processing areas during covert and overt tracking tasks. Neuroimage 41:380–388.

Albright TD, Stoner GR. 1995. Visual motion perception. Proc Natl Acad Sci U S A 92:2433–2440.

Angelaki DE, Cullen KE. 2008. Vestibular system: the many facets of a multimodal sense. Annu Rev Neurosci 31:125–150.

Angelucci A, Levitt JB, Walton EJ, Hupe JM, Bullier J, Lund JS. 2002. Circuits for local and global signal integration in primary visual cortex. J Neurosci 22:8633–8646.

Anker AR, Ali A, Arendt HE, Cass SP, Cotter LA, Jian BJ, et al. 2003. Use of electrical vestibular stimulation to alter genioglossal muscle activity in awake cats. J Vestib Res 13:1–8.

Baloh RW, Honrubia V. 1990. *Clinical neurophysiology of the vestibular system*. Philadelphia: F.A. Davis Company.

Bense S, Stephan T, Bartenstein P, Schwaiger M, Brandt T, Dieterich M. 2005. Fixation suppression of optokinetic nystagmus modulates cortical visual-vestibular interaction. Neuroreport 16:887.

Bense S, Janusch B, Vucurevic G, Bauermann T, Schlindwein P, Brandt T, et al. 2006. Brainstem and cerebellar fMRI-activation during horizontal and vertical optokinetic stimulation. Exp Brain Res 174:312–323.

Beraneck M, Cullen KE. 2007. Activity of vestibular nuclei neurons during vestibular and optokinetic stimulation in the alert mouse. J Neurophysiol 98:1549–1565.

Berman RA, Wurtz RH. 2010. Functional identification of a pulvinar path from superior colliculus to cortical area MT. J Neurosci 30:6342–6354.

Bicchi A, Scilingo EP, Ricciardi E, Pietrini P. 2008. Tactile flow explains haptic counterparts of common visual illusions. Brain Res Bull 75:737–741.

Blazquez PM, Highstein SM. 2007. Visual-vestibular interaction in vertical vestibular only neurons. Neuroreport 18:1403–1406.

Bolognini N, Pascual-Leone A, Fregni F. 2009 Using non-invasive brain stimulation to augment motor training-induced plasticity. J Neuroeng Rehabil 6:6–8.

Borel L, Lopez C, Péruch P, Lacour M. 2008. Vestibular syndrome: a change in internal spatial representation. Neurophysiol Clin 38:375–389.

Brandt T, Dieterich M. 1999. The vestibular cortex: its locations, functions, and disorders. Ann N Y Acad Sci 871:293–312.

Brandt T, Bartenstein P, Janek A, Dieterich M. 1998 Reciprocal inhibitory visual-vestibular interaction. Visual motion stimulation deactivates the parieto-insular vestibular cortex. Brain 121:1749–1758.

Brandt T, Glasauer S, Stephan T, Bense S, Yousry TA, Deutschlander A, et al. 2002. Visual-vestibular and visuovisual cortical interaction: new insights from fMRI and pet. Ann N Y Acad Sci 956:230–241.

Buisseret-Delmas C, Compoint C, Delfini C, Buisseret P. 1999. Organisation of reciprocal connections between trigeminal and vestibular nuclei in the rat. J Comp Neurol 409:153–168.

Cardin V, Smith AT. 2010. Sensitivity of human visual and vestibular cortical regions to egomotion-compatible visual stimulation. Cereb Cortex 20:1964–1973.

Chumbley JR, Friston KJ, Fearn T, Kiebel SJ. 2007. A metropolis-hastings algorithm for dynamic causal models. Neuroimage 38:478–487.

Cox RW. 1996. AFNI: Software for analysis and visualization of functional magnetic resonance neuroimages. Comput Biomed Res 29:162–173.

Curthoys IS, Halmagyi GM. 1995. Vestibular compensation: a review of the oculomotor, neural, and clinical consequences of unilateral vestibular loss. J Vestib Res 5:67–107.

Danilov Y, Tyler M, Skinner K, Hogle R, Bach-y-Rita P. 2007. Efficacy of electrotactile vestibular substitution in patients with peripheral and central vestibular loss. J Vestib Res 17:119–130.

Danilov Y, Tyler M. 2005. Brainport: an alternative input to the brain. J Integr Neurosci 4:537–550.

Danilov YP, Tyler ME, Skinner KL, Bach-y-Rita P. 2006. Efficacy of electrotactile vestibular substitution in patients with bilateral vestibular and central balance loss. Conf Proc IEEE Eng Med Biol Soc Suppl:6605–6609.

de Marco G, Vrignaud P, Destrieux C, de Marco D, Testelin S, Devauchelle B, et al. 2009. Principle of structural equation modeling for exploring functional interactivity within a putative network of interconnected brain areas. Magn Reson Imaging 27:1–12.

Dieterich M. 2007. Central vestibular disorders. J Neurol 254:559–568.

Dieterich M, Brandt T. 2000. Brain activation studies on visual-vestibular and ocular motor interaction. Curr Opin Neurol 13:13–18.

Dieterich M, Bauermann T, Best C, Stoeter P, Schlindwein P. 2007. Evidence for cortical visual substitution of chronic bilateral vestibular failure (an fMRI study). Brain 130:2108–2116.

Dieterich M, Bense S, Stephan T, Yousry TA, Brandt T. 2003. fMRI signal increases and decreases in cortical areas during small-field optokinetic stimulation and central fixation. Exp Brain Res 148:117–127.

Dieterich M, Brandt T. 2008. Functional brain imaging of peripheral and central vestibular disorders. Brain 131:2538–2552.

DuBois Bowman F, Caffo B, Bassett SS, Kilts C. A 2008. bayesian hierarchical framework for spatial modeling of fMRI data. Neuroimage 39:146–156.

Eickhoff SB, Weiss PH, Amunts K, Fink GR, 2006. Zilles K. Identifying human parieto-insular vestibular cortex using fMRI and cytoarchitectonic mapping. Hum Brain Mapp 27:611–621.

Fetsch CR, Turner AH, DeAngelis GC, Angelaki DE. 2009. Dynamic reweighting of visual and vestibular cues during self-motion perception. J Neurosci 29:15601.

Fries W. 1990. Pontine projection from striate and prestriate visual cortex in the macaque monkey: an anterograde study. Vis Neurosci 4:205–216.

Friston KJ, Harrison L, Penny W. 2003. Dynamic causal modelling. Neuroimage 19:1273–1302.

Friston KJ, Buchel C. 2000. Attentional modulation of effective connectivity from V2 to V5/MT in humans. Proc Natl Acad Sci U S A 97:7591–7596.

Greenlee MW, Tse PU. 2008. Functional neuroanatomy of the human visual system: a review of functional MRI studies. In: Lorenz B, Borruat FX (eds.) Pediatric Ophthalmology, Neuro-Ophthalmology, Genetics. Berlin Heidelberg: Springer; pp. 119–138.

Guerraz M, Bronstein AM. 2008. Ocular versus extraocular control of posture and equilibrium. Neurophysiol Clin 38:391–398.

Herrick JL, Keifer J. 2000. Central trigeminal and posterior eighth nerve projections in the turtle chrysemys picta studied in vitro. Brain Behav Evol 51:183–201.

Hesterberg T, Monaghan S, Moore DS, Clipson A, Epstein R. 2008. Bootstrapping methods and permutation tests. In: Moore DS, McCabe GP, Duckworth II WM, Alwin L (eds.) The Practice of Business Statistics. New York, NY: W.H. Freeman; p. 859.

Indovina I, Maffei V, Bosco G, Zago M, Macaluso E, Lacquaniti F. 2005. Representation of visual gravitational motion in the human vestibular cortex. Science 308:416–419.

Kaczmarek KA. 2011. The tongue display unit for electrotactile spatiotemporal pattern presentation. Sci Iran D 18:1476–1485.

Kasess CH, Stephan KE, Weissenbacher A, Pezawas L, Moser E, Windischberger C. 2010. Multi-subject analyses with dynamic causal modeling. Neuroimage 49:3065–3074.

Kikuchi M, Naito Y, Senda M, Okada T, Shinohara S, Fujiwara K, et al. 2009. Cortical activation during optokinetic stimulation - an fMRI study. Acta Otolaryngol 129:440–443.

Kovacs G, Raabe M, Greenlee MW. 2008. Neural correlates of visually induced self-motion illusion in depth. Cereb Cortex 18:1779–1787.

Lanyon LJ, Giaschi D, Young SA, Fitzpatrick K, Diao L, Bjornson BH, et al. 2009. Combined functional MRI and diffusion tensor imaging analysis of visual motion pathways. J Neuro-Ophthalmol 29:96–103.

Lewis JW, Beauchamp MS, DeYoe EA. 2000. A comparison of visual and auditory motion processing in human cerebral cortex. Cereb Cortex 10:873–888.

Lockhart RA, O'Reilly FJ, Stephens MA. 2007. Use of gibbs sampler to obtain conditional tests, with aplications. Biometrika 94:992–998.

Lopez C, Blanke O. 2011. The thalamocortical vestibular system in animals and humans. Brain Res Rev 67:119–146.

Mahboobin A, Loughlin PJ, Redfern MS, Sparto PJ. 2005. Sensory re-weighting in human postural control during moving-scene perturbations. Exp Brain Res 167:260–267.

Mandonnet E, Winkler PA, Duffau H. 2010. Direct electrical stimulation as an input gate into brain functional networks: principles, advantages and limitations. Acta Neurochir (Wien) 152:185–193.

Marano E, Marcelli V, Stasio ED, Bonuso S, Vacca G, Manganelli F, et al 2005.. Trigeminal stimulation elicits a peripheral vestibular imbalance in migraine patients. Headache J Head Face Pain 45:325–331.

Matteau I, Kupers R, Ricciardi E, Pietrini P, Ptito M. 2010. Beyond visual, aural and haptic movement perception: HMT + is activated by electrotactile motion stimulation of the tongue in sighted and in congenitally blind individuals. Brain Res Bull 82:264–270.

McKeefry DJ, Gouws A, Burton MP, Morland AB. 2009. The non-invasive dissection of the human visual cortex: Using FMRI and TMS to study the organization of the visual brain. Neuroscientist 15:489–506.

Ohlendorf S, Sprenger A, Speck O, Haller S, Kimmig H. 2008. Optic flow stimuli in and near the visual field centre: a group fMRI study of motion sensitive regions. PLoS ONE 3: e4043.

Penny WD, Stephan KE, Mechelli A, Friston KJ. 2004. Comparing dynamic causal models. Neuroimage 22:1157–1172.

Penny WD, Stephan KE, Daunizeau J, Rosa MJ, Friston KJ, Schofield TM, et al. 2010. Comparing families of dynamic causal models. PLoS Comput Biol 6: e1000709.

Previc FH, Liotti M, Blakemore C, Beer J, Fox P. 2000. Functional imaging of brain areas involved in the processing of coherent and incoherent wide field-of-view visual motion. Exp Brain Res 131:393–405.

Ptito M, Moesgaard SM, Gjedde A, Kupers R. 2005. Cross-modal plasticity revealed by electrotactile stimulation of the tongue in the congenitally blind. Brain 128:606.

Redfern MS, Furman JM. 1994. Postural sway of patients with vestibular disorders during optic flow. J Vestib Res 4:221–230.

Redfern MS, Yardley L, Bronstein AM. 2001. Visual influences on balance. J Anxiety Disord 15:81–94.

Ricciardi E, Vanello N, Sani L, Gentili C, Scilingo EP, Landini L, et al. 2007. The effect of visual experience on the development of functional architecture in hMT+. Cereb Cortex 17:2933–2939.

Roebroeck A, Formisano E, Goebel R. 2005. Mapping directed influence over the brain using granger causality and fMRI. Neuroimage 25:230–242.

Sampaio E, Maris S, Bach-y-Rita P. 2001. Brain plasticity: "visual"acuity of blind persons via the tongue. Brain Res 908:204–207.

Sathian K. 2005. Visual cortical activity during tactile perception in the sighted and the visually deprived. Dev Psychobiol 46:279–286.

Satoh Y, Ishizuka KI, Murakami T. 2009. Modulation of the masseteric monosynaptic reflex by stimulation of the vestibular nuclear complex in rats. Neurosci Lett 466:16–20.

Schoenfeld MA, Heinze HJ, Woldorff MG. 2002. Unmasking motion-processing activity in human brain area V5/MT+ mediated by pathways that bypass primary visual cortex. Neuroimage 17:769–779.

Schumacker RE, Lomax RG. 1996. *A Beginner's Guide to Structural Equation Modeling*. New Jersey: Mahwah.

Sincich LC, Park KF, Wohlgemuth MJ, Horton JC. 2004. Bypassing V1: a direct geniculate input to area MT. Nat Neurosci 7:1123–1128.

Slobounov S, Wu T, Hallett M, Shibasaki H, Slobounov E, Newell K. 2006. Neural underpinning of postural responses to visual field motion. Biol Psychol 72:188–197.

Stephan KE, Penny WD, Daunizeau J, Moran RJ, Friston KJ. 2009. Bayesian model selection for group studies. Neuroimage 46:1004–1017.

Stephan KE, Kasper L, Harrison LM, Daunizeau J, den Ouden HE, Breakspear M, et al. 2008. Nonlinear dynamic causal models for fMRI. Neuroimage 42:649–662.

Sunaert S, Van Hecke P, Marchal G, Orban GA. 1999. Motion-responsive regions of the human brain. Exp Brain Res 127:355–370.

Suzuki M, Kitano H, Ito R, Kitanishi T, Yazawa Y, Ogawa T, et al. 2001. Cortical and subcortical vestibular response to caloric stimulation detected by functional magnetic resonance imaging. Cogn Brain Res 12:441–449.

Tyler M, Danilov Y, Bach-Y-Rita P. 2003. Closing an open-loop control system: Vestibular substitution through the tongue. J Integr Neurosci 2:159–164.

Vuillerme N, Cuisinier R. 2009. Sensory supplementation through tongue electrotactile stimulation to preserve head stabilization in space in the absence of vision. Invest Ophthalmol Vis Sci 50:476–481.

Wall JT, Symonds LL, Kaas JH. 1982. Cortical and subcortical projections of the middle temporal area (MT) and adjacent cortex in galagos. J Comp Neurol 211:193–214.

Wildenberg JC, Tyler ME, Danilov YP, Kaczmarek KA, Meyerand ME. 2011a. High-resolution fMRI detects neuromodulation of individual brainstem nuclei by electrical tongue stimulation in balance-impaired individuals. Neuroimage 56:2129–2137.

Wildenberg JC, Tyler ME, Danilov YP, Kaczmarek KA, Meyerand ME. 2011b. Electrical tongue stimulation normalizes activity within the motion-sensitive brain network in balance-impaired subjects as revealed by group independent component analysis. Brain Connectivity 1:265.

Wildenberg JC, Tyler ME, Danilov YP, Kaczmarek KA, Meyerand ME. 2010. Sustained cortical and subcortical neuromodulation induced by electrical tongue stimulation. Brain Imaging Behav 4:199–211.

Address correspondence to:
Joe C. Wildenberg
Neuroscience Training Program
1129, Wisconsin Institute for Medical Research
University of Wisconsin
1111 Highland Avenue
Madison, WI 53705

E-mail: joe.wildenberg@gmail.com